



Supplement of

Decadal changes in anthropogenic source contribution of PM_{2.5} pollution and related health impacts in China, 1990–2015

Jun Liu et al.

Correspondence to: Qiang Zhang (qiangzhang@tsinghua.edu.cn)

The copyright of individual parts of the supplement might differ from the CC BY 4.0 License.

Validation of WRF-CMAQ modelling system

The domain-wide meteorological evaluation was carried out with the observed hourly surface temperature, relative humidity, wind speed, wind direction from the National Climate Data Center (www.ncdc.noaa.gov/) dataset. The evaluation parameters include mean bias (MB), root mean square error (RMSE), mean error (ME), normalized mean bias (NMB), normalized mean error (NME), and correlation coefficient (R). More than 1500 meteorological stations were located in the simulation domain. Table S1 shows the performance statistics in details. In general, the WRF model performed consistently over the past twenty-five years, and model performances were comparable among different years. The 2-m temperature agreed well with observations with the MB and RMSE ranging at -0.3~-0.1K and 2.6~2.8K, respectively. For 2-m relative humidity, the MB and NMB were 3.3~3.9% and 4.7~5.7%, respectively, showing close agreements between the simulations and observations. The simulated 10-m wind speed and the 10-m wind direction agreed fairly close with observations. Overall, the WRF model performed reasonably well during the simulation years, and the performance statistics are comparable with previous WRF-CMAQ (Hu et al. 2016; Zheng et al. 2015) and WRF-Chem (Liu et al. 2016) simulations over China.

Since 2013, direct PM_{2.5} measurements have been included in China National Monitoring Network. Therefore, we conducted a detailed CMAQ model evaluation for year 2015. Daily PM_{2.5} observations at 495 stations in 74 major cities were derived from monitoring data published the China National Environmental Monitoring Center (CNEMC, <http://106.37.208.233:20035>). Simulated hourly concentrations in the surface grid cell at the measurement location were used to derive the daily average concentrations. The averages of observations and simulations of PM_{2.5} for each city are used for model evaluation. For the entire year, the average observed and simulated PM_{2.5} concentrations were 54.4 $\mu\text{g m}^{-3}$ and 59.4 $\mu\text{g m}^{-3}$, with correlation coefficient, RMSE, NMB at 0.73, 34.2 $\mu\text{g m}^{-3}$ and 9.1%, respectively, indicating good agreements between observations and simulations. Figure S2 shows the overlay of observed and simulated seasonal PM_{2.5} concentrations. Spatially, high PM_{2.5} concentrations were distributed in Eastern and Central China, with concentration peaks in the Beijing-Tianjin-Hebei and the surrounding regions. There were obvious seasonal variations in PM_{2.5}, with the highest concentration in winter, and lowest concentration in Summer. Compared with the observations, the modelling system well reproduced the spatial and seasonal pattern of PM_{2.5} in most of the regions over China, but underestimated the PM_{2.5} concentrations in the west, where the dust source region was located.

Besides, to provide a view for other years, we compared the CMAQ simulated anthropogenic PM_{2.5} with the satellite-derived dust-free PM_{2.5} from van Donkelaar et al. (2016) for all the overlapping years, including 2000, 2005, 2010 and 2015 (Figure S3). In general, the CMAQ simulated anthropogenic PM_{2.5} has a good correlation with satellite-derived dust-free PM_{2.5}, with R² ranging from 0.76 to 0.86. Better agreements occurred in recent years, especially in 2015, when direct PM_{2.5} measurements were available to evaluate the CMAQ model and calibrate the satellite-based estimates. Higher PM_{2.5} estimates from CMAQ occurred in early years, such as 2000, indicating larger uncertainties in exposure estimates for these early years. Since the satellite-based PM_{2.5} estimates have their own uncertainties, it's unknown which estimate is more

reliable. However, since we focus more on the relative contribution of different source sectors in this study, the uncertainties from exposure estimates could be partially offset by the division operation.

References

- Hu J, Chen J, Ying Q, Zhang H. 2016. One-year simulation of ozone and particulate matter in China using WRF/CMAQ modeling system. *Atmos Chem Phys* 16:10333–10350; doi:10.5194/acp-16-10333-2016.
- Liu J, Mauzerall DL, Chen Q, Zhang Q, Song Y, Peng W, et al. 2016. Air pollutant emissions from Chinese households: A major and underappreciated ambient pollution source. *Proc Natl Acad Sci* 113:7756–7761; doi:10.1073/pnas.1604537113.
- van Donkelaar, A., Martin, R. V., Brauer, M., Hsu, N. C., Kahn, R. A., Levy, R. C., Lyapustin, A., Sayer, A. M. and Winker, D. M.: Global Estimates of Fine Particulate Matter using a Combined Geophysical-Statistical Method with Information from Satellites, Models, and Monitors, *Environ. Sci. Technol.*, 50(7), 3762–3772, doi:[10.1021/acs.est.5b05833](https://doi.org/10.1021/acs.est.5b05833), 2016.
- Zheng B, Zhang Q, Zhang Y, He KB, Wang K, Zheng GJ, et al. 2015. Heterogeneous chemistry: a mechanism missing in current models to explain secondary inorganic aerosol formation during the January 2013 haze episode in North China. *Atmospheric Chem Phys* 15:2031–2049; doi:10.5194/acp-15-2031-2015.

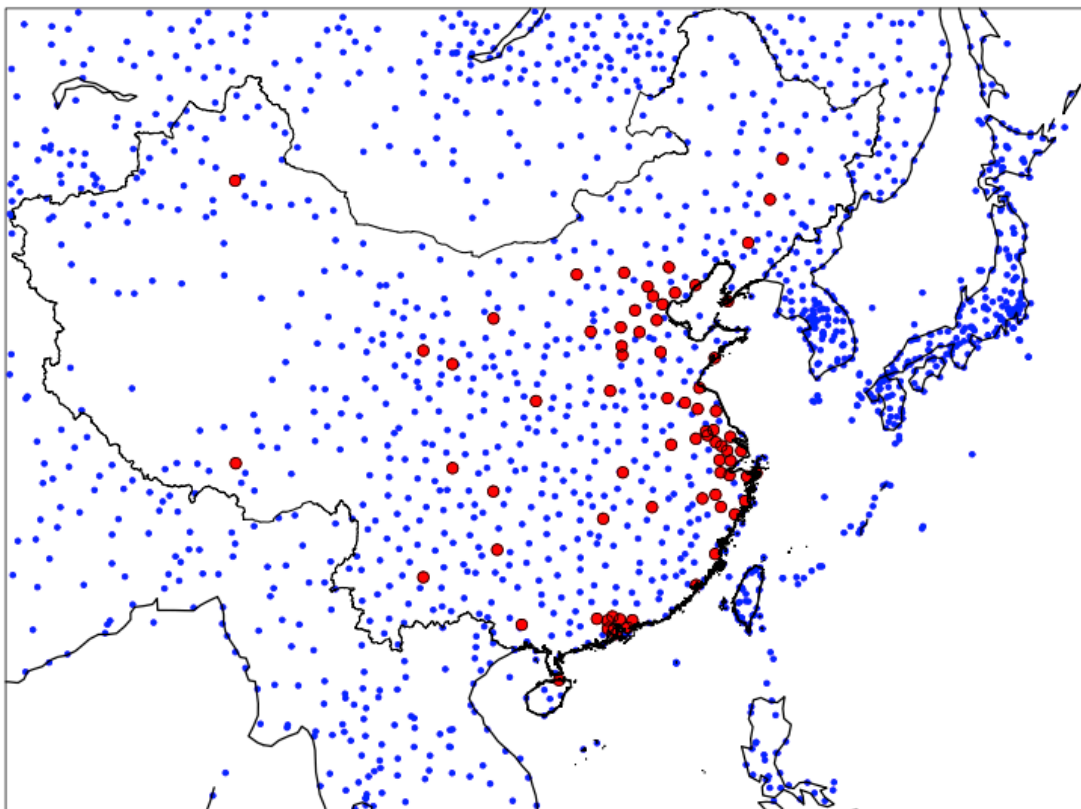


Figure S1: Domain used in WRF-CMAQ and location of monitoring stations for model evaluation. Blue dots are the meteorological sites included in the National Climate Data Center dataset, and red dots are the location of 74 major cities with monitoring stations included in the China National Monitoring Network for PM_{2.5} concentrations.

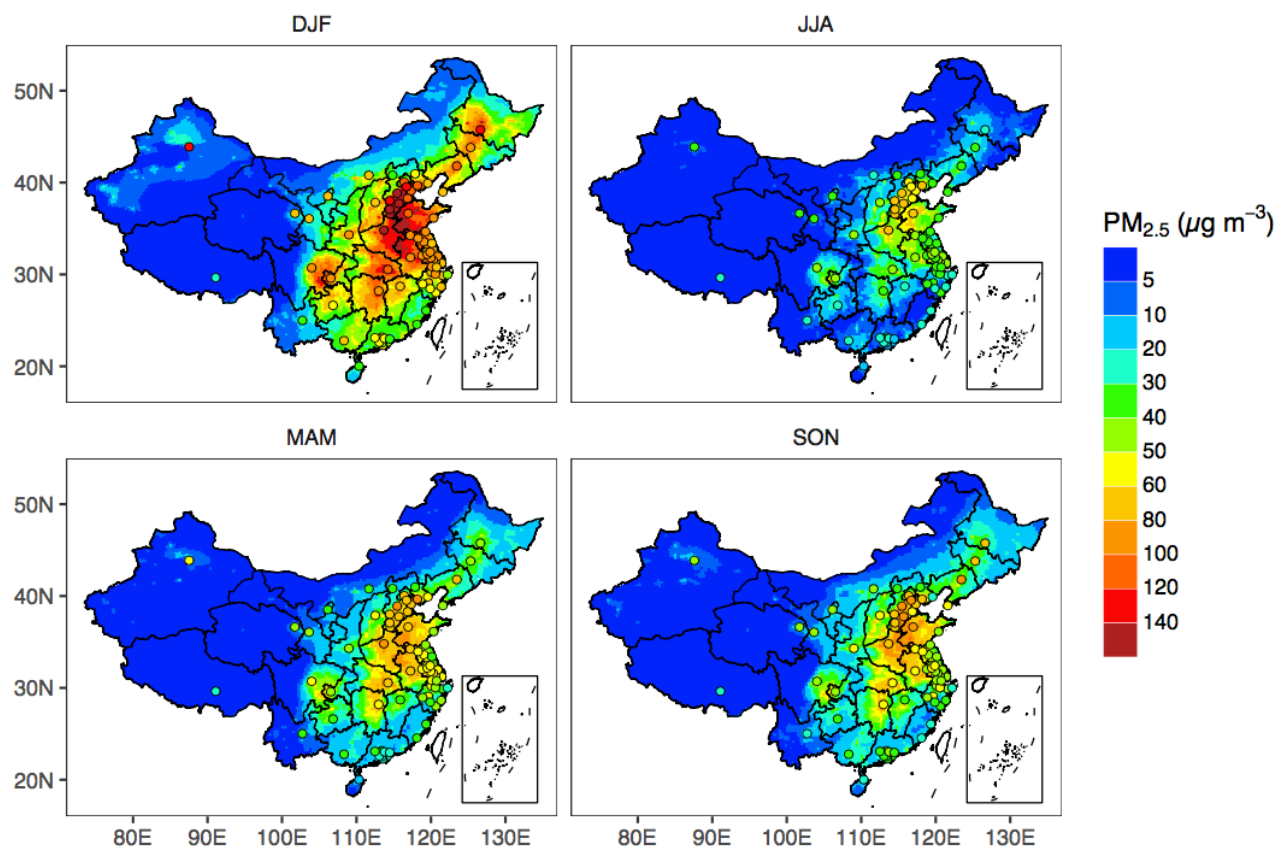


Figure S2: Simulated and observed seasonal average $PM_{2.5}$ concentration in 74 cities in China.

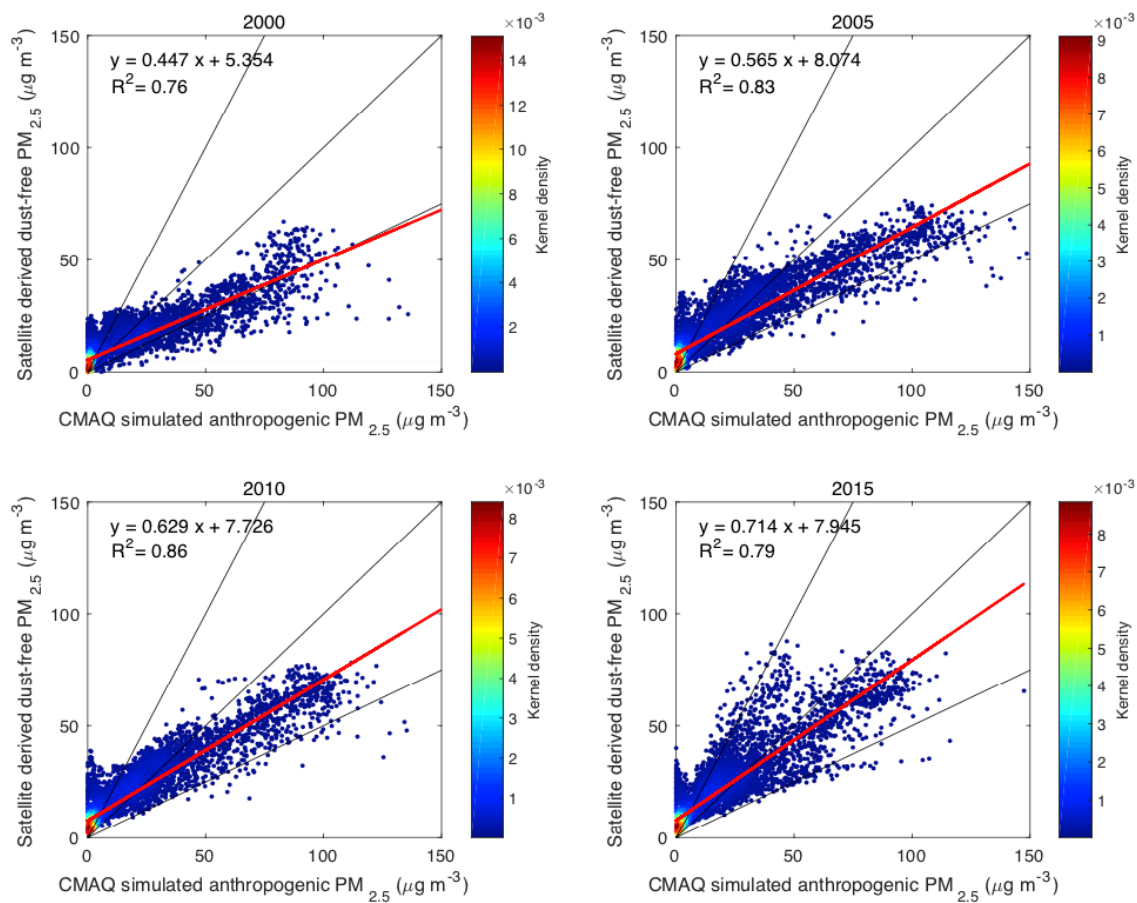


Figure S3: Comparison of CMAQ simulated anthropogenic $PM_{2.5}$ and satellite derived dust-free $PM_{2.5}$ in China (the dots are colored with the kernel density estimate)

Year	Power	Industry		Transportation	
		Cement	Iron and steel	Light-duty gasoline	Heavy-duty diesel
1990	Pre-stage	GB4915-1985	GB9078-1988	Pre-stage	Pre-stage
1991	GB13223-1991				
1992					
1993					
1994					
1995					
1996					
1997	GB13223-1996	GB4915-1996	GB 9078-1996	Euro I	Euro I
1998					
1999					
2000					
2001					
2002					
2003	GB13223-2003	GB4915-2004		Euro II	Euro II
2004					
2005					
2006					
2007					
2008					
2009	GB13223-2011	GB4915-2013	GB28662-2012 GB28663-2012 GB28664-2012 GB28665-2012	Euro III	Euro III
2010					
2011					
2012					
2013					
2014					
2015				Euro IV	Euro IV

Figure S4: Emission standards implemented in major sectors during 1990-2015.

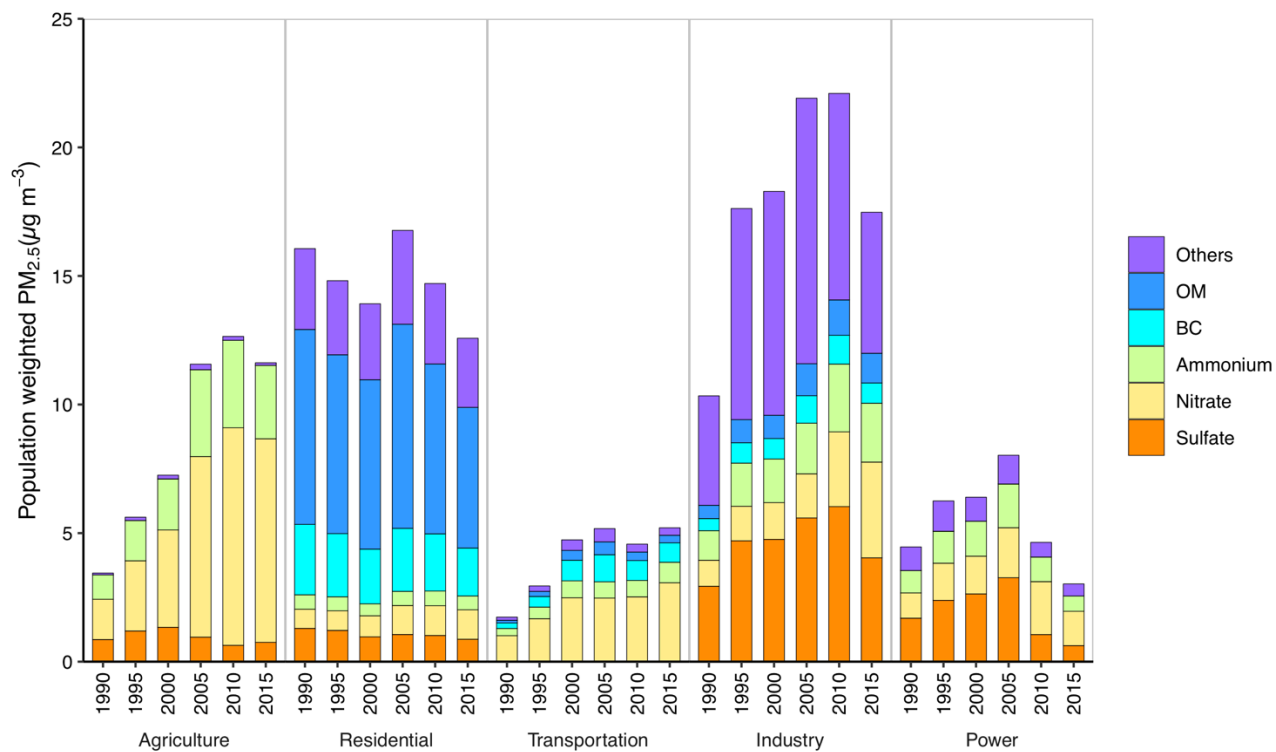


Figure S5: Chemical composition of the population-weighted $PM_{2.5}$ concentrations by source sectors during 1990-2015.

Table S1: Performance statistics for meteorological fields simulated by WRF

year	Meteorological field	Data Pairs	R	Observed mean	Simulated mean	MB	RMSE	ME	NMB (%)	NME (%)
2000	2-m temperature (K)	4192027	0.98	13.6	13.5	-0.1	2.8	2.0	-0.6	14.4
	2-m relative humidity (%)	4178440	0.79	70.5	73.8	3.3	12.8	9.4	4.7	13.4
	10-m wind speed (m/s)	4150033	0.57	2.8	2.8	0.0	2.1	1.5	0.7	55.2
	10-m wind direction (°)	3513773	0.41	193.9	190.9	1.9	64.2	46.6	1.0	24.0
2005	2-m temperature (K)	4747580	0.98	13.8	13.6	-0.2	2.7	1.9	-1.2	13.8
	2-m relative humidity (%)	4737573	0.81	68.8	72.8	3.9	12.6	9.4	5.7	13.7
	10-m wind speed (m/s)	4741462	0.60	2.8	2.9	0.1	2.0	1.5	3.7	53.5
	10-m wind direction (°)	4087836	0.42	194.8	196.8	1.8	64.6	46.7	0.9	24.0
2010	2-m temperature (K)	5099963	0.98	14.2	14.0	-0.2	2.6	1.8	-1.2	12.9
	2-m relative humidity (%)	5090225	0.82	69.5	73.2	3.7	12.1	9.1	5.3	13.0
	10-m wind speed (m/s)	5093539	0.53	2.7	3.1	0.4	2.2	1.6	14.4	60.6
	10-m wind direction (°)	4368053	0.38	191.0	197.5	0.8	68.8	50.6	0.4	26.5
2015	2-m temperature (K)	5153973	0.98	14.9	14.5	-0.3	2.7	1.9	-2.3	13.0
	2-m relative humidity (%)	5145148	0.82	69.9	73.7	3.8	12.6	9.5	5.4	13.5
	10-m wind speed (m/s)	4924354	0.61	2.8	2.8	0.1	1.9	1.4	2.8	50.8
	10-m wind direction (°)	4165012	0.40	193.6	188.5	2.0	65.7	47.6	1.0	24.6